Inorg. Chem. **2008**, *47*, 5992−6000

Inorganic Chemistry
Article

Synthesis and Characterization of Aluminum- and Gallium-Bridged [1.1]Chromarenophanes and [1.1]Molybdarenophanes

Clinton L. Lund,[†] Jörg A. Schachner,[†] Ian J. Burgess,[†] J. Wilson Quail,[‡] Gabriele Schatte,[‡] and Jens Müller*[,†]

Department of Chemistry and Saskatchewan Structural Sciences Centre, University of Saskatchewan, 110 Science Place, Saskatoon, Saskatchewan S7N 5C9, Canada

Received February 21, 2008

The synthesis and structural characterization of the first [1.1]chromarenophanes and the first [1.1]molybdarenophanes are described. A salt-metathesis reaction of [2-(Me_2NCH_2)C_6H_4]$AlCl_2$ with freshly prepared [Cr(LiC_6H_5)$_2$] · TMEDA (TMEDA = *N*,*N*,*N*′,*N*′-tetramethylethylenediamine) resulted in the dialumina[1.1]chromarenophane [{2-(Me_2NCH_2)-C_6H_4}Al(η^6-C_6H_5)$_2$Cr]$_2$ (**2a**). The poor solubility of **2a** in organic solvents prompted us to synthesize the new intramolecularly coordinated aluminum- and gallium dichlorides [5-*t*Bu-2-(Me_2NCH_2)C_6H_3]ECl_2 [E = Al (**3a**), Ga (**3b**)] in which the phenyl group was equipped with a *tert*-butyl group. Salt-metathesis reactions of **3a** and **3b**, respectively, with freshly prepared [M(LiC_6H_5)$_2$] · TMEDA (M = Cr, Mo) resulted in four new [1.1]metallarenophanes of the general type [{5-*t*Bu-2-(Me_2NCH_2)C_6H_3}E(η^6-C_6H_5)$_2$M]$_2$ [E = Al, M = Cr (**4a**); *E* = Ga, M = Cr (**4b**); E = Al, M = Mo (**5a**); E = Ga, M = Mo (**5b**)]. **2a**, **4a**,**b**, and **5a**,**b** have been structurally characterized by single-crystal analysis [**2a** · 1/2C_6H_{12}: $C_{48}H_{56}Al_2Cr_2N_2$, monoclinic, $P2_1/c$, a = 9.9117(9) Å, b = 19.9361(16) Å, c = 10.638(2) Å, α = 90°, β = 112.322(5)°, γ = 90°, Z = 2; **4a** · 2C_6H_6: $C_{62}H_{72}Al_2Cr_2N_2$, monoclinic, $P2_1/c$, a = 10.9626(9) Å, b = 19.3350(18) Å, c = 12.4626(9) Å, α = 90°, β = 100.756(5)°, γ = 90°, Z = 2; **4b** · 2C_6H_6: $C_{62}H_{72}Cr_2Ga_2N_2$, monoclinic, $P2_1/c$, a = 10.8428(2) Å, b = 19.4844(4) Å, c = 12.4958(2) Å, α = 90°, β = 100.6187°, γ = 90°, Z = 2; **5a** · 2C_6H_6: $C_{62}H_{72}Al_2Mo_2N_2$, triclinic, $P\bar{1}$, a = 10.4377(4) Å, b = 11.6510(4) Å, c = 11.6514(4) Å, α = 73.545(3)°, β = 89.318(2)°, γ = 76.120(2)°, Z = 1; **5b** · 2C_6H_6: $C_{62}H_{72}Ga_2Mo_2N_2$, triclinic, $P\bar{1}$, a = 10.3451(5) Å, b = 11.6752(6) Å, c = 11.6900(5) Å, α = 73.917(3)°, β = 89.550(3)°, γ = 76.774(2)°, Z = 1]. All five [1.1]metallarenophanes **2a**, **4a**,**b**, and **5a**,**b** crystallize as anti isomers with both Me_2N donor groups in exo positions (C_i point group symmetry). The new [1.1]metallarenophanes show NMR spectra that can be interpreted as being caused by time-averaged C_{2h} symmetrical species, which is consistent with the findings of their molecular structures in the solid state. Variable-temperature ^{1}H NMR measurements for **4a**,**b** and **5a**,**b** (500 MHz; −90 to 90 °C) revealed only peak broadening in the lower temperature range of −70 to −90 °C. ^{1}H NMR saturation transfer difference experiments did not show an expected anti-to-anti isomerization, rendering the new [1.1]metallacyclophanes rigid on the NMR time scale. Electrochemical measurements were performed for **4a**,**b** and **5a**,**b**. However, reproducible cyclic voltammograms could only be obtained for the two gallium species **4b** and **5b**, revealing the expected weak communication between the two transition-metal atoms in both compounds (class II).

Introduction

Since their first appearance in the literature in 1966,[1] [1.1]ferrocenophanes have been the subject of intensive investigations. The chemistry of the carbon-bridged [1.1]ferrocenophanes was reviewed in 1986 by Mueller-Westerhoff.[2] Usually, carbon-bridged [1.1]ferrocenophanes prefer the syn conformation (Figure 1, E = C); however, in 1993 the first structural evidence for the existence of the second isomer, the anti isomer (Figure 1), was reported.[3] In this particular case, CHMe moieties bridged the two ferrocene units and

---

* To whom correspondence should be addressed. E-mail: jens.mueller@usask.ca.

[†] Department of Chemistry, University of Saskatchewan.

[‡] Saskatchewan Structural Sciences Centre, University of Saskatchewan.

(1) Watts, W. E. *J. Am. Chem. Soc.* **1966**, *88*, 855–856.

(2) Mueller-Westerhoff, U. T. *Angew. Chem., Int. Ed. Engl.* **1986**, *25*, 702–717.

10.1021/ic800336f CCC: $40.75

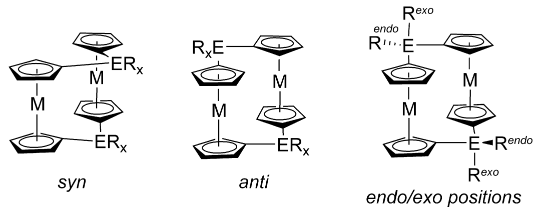

Figure 1. Isomerism in [1.1]metallocenophanes.

gave rise to endo/exo isomers (Figure 1). [1.1]Ferrocenophanes are highly dynamic in solution and have been coined "molecular acrobats".[2,4] A distanna[1.1]ferrocenophane (E = SnBu$_2$)[5] was the first heteroatom bridged [1.1]ferrocenophane and since its discovery, the group of heteroatom containing [1.1]ferrocenophanes has grown significantly and is now known for groups 13 (boron,[6] aluminum,[7–9] gallium,[9,10] indium,[9]), 14 (silicon,[11,12] tin,[5,13] lead[14]), 15 (phosphorus[15]), and 16 (sulfur[16]).

The knowledge about [1.1]ruthenocenophanes and mixed Ru−Fe [1.1]metallocenophanes is mainly limited to carbon-bridged species, with the knowledge about heteroatom-bridged [1.1]ruthenocenophane being limited to a SiMe$_2$-bridged species published in 1995 by Herberhold et al.[12]

In the course of our investigation into strained [1]metallacyclophanes with heavier group 13 elements in bridging positions,[17] we found that dilithioferrocene reacts with intramolecularly coordinated group 13 element halides Ar′EX$_2$ (Ar′ = 2-(Me$_2$NCH$_2$)C$_6$H$_4$; E = Al,[8,9] Ga,[9] In[9]) to give [1.1]ferrocenophanes. Even though [1.1]ferrocenophanes are unstrained and, therefore, cannot be used for ring-opening polymerizations, they serve as model compounds for the investigation of metal−metal interactions. Using cyclic voltammetry, we have shown that two isostructural [1.1]ferrocenophanes, a gallium- and an aluminum-bridged species, show distinctively different redox behavior. Whereas the digalla[1.1]ferrocenophane[9] showed the expected class II[18] behavior (two one-electron oxidation waves) similar to other [1.1]ferrocenophanes, the dialumina[1.1]ferrocenophane[9] showed an unexpected class I[18] behavior (one two-electron oxidation wave). On the basis of these findings, we wanted to explore reactions of other dilithio sandwich compounds with intramolecularly coordinated alanes and gallanes of the type Ar′EX$_2$. We were hoping to obtain [1.1]metallacyclophanes to further investigate metal−metal interactions.

In contrast to the large number of [1.1]metallocenophanes, it is surprising that not a single example of a [1.1]metallarenophane is described in the literature. Within this article, we fill this gap by reporting on the synthesis and characterization of the first [1.1]chromarenophanes and the first [1.1]molybdarenophanes.

Results and Discussion

We started to investigate the reaction of dilithiobis(benzene)chromium with Ar′AlCl$_2$ (**1a**). After several attempts using various reaction conditions, we obtained red crystals from this reaction (eq 1). Interestingly, once **2a** crystallized it could not be redissolved in common organic solvents.

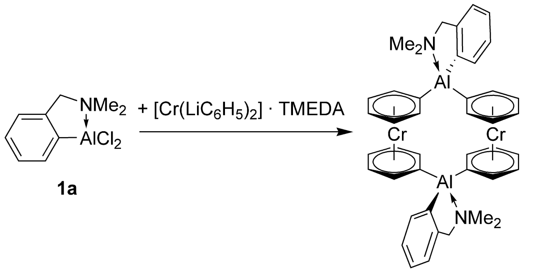

1a

2a

(1)

However, the compound is sparingly soluble in THF, and a small amount of single crystals of sufficient quality for X-ray single-crystal analysis were obtained from highly diluted THF solution in the presence of cyclohexane (Figure 2, Table 1). The structural analysis clearly revealed that **2a** is a [1.1]chromarenophane. To the best of our knowledge, it

---

[3] Löwendahl, M.; Davidsson, Ö.; Ahlberg, P.; Håkansson, M. *Organometallics* **1993**, *12*, 2417–2419.

[4] Löwendahl, M.; Davidsson, Ö.; Ahlberg, P. *J. Chem. Res., Synop.* **1993**, *4*, 0–41.

[5] Clearfield, A.; Simmons, C. J., Jr.; Seyferth, D. *Inorg. Chim. Acta* **1983**, *75*, 139–144.

[6] Scheibitz, M.; Winter, R. F.; Bolte, M.; Lerner, H.-W.; Wagner, M. *Angew. Chem., Int. Ed.* **2003**, *42*, 924–927.

[7] Schachner, J. A.; Lund, C. L.; Quail, J. W.; Müller, J. *Acta Crystallogr.* **2005**, *E61*, m682−m684.

[8] Braunschweig, H.; Burschka, C.; Clentsmith, G. K. B.; Kupfer, T.; Radacki, K. *Inorg. Chem.* **2005**, *44*, 4906–4908.

[9] Schachner, J. A.; Orlowski, G. A.; Quail, J. W.; Kraatz, H.-B.; Müller, J. *Inorg. Chem.* **2006**, *45*, 454–459.

[10] (a) Jutzi, P.; Lenze, N.; Neumann, B.; Stammler, H. G. *Angew. Chem., Int. Ed.* **2001**, *40*, 1424–1427. (b) Uhl, W.; Hahn, I.; Jantschak, A.; Spies, T. *J. Organomet. Chem.* **2001**, *637*, 300–303. (c) Althoff, A.; Jutzi, P.; Lenze, N.; Neumann, B.; Stammler, A.; Stammler, H.-G. *Organometallics* **2002**, *21*, 3018–3022. (d) Althoff, A.; Jutzi, P.; Lenze, N.; Neumann, B.; Stammler, A.; Stammler, H. G. *Organometallics* **2003**, *22*, 2766–2774. (e) Althoff, A.; Eisner, D.; Jutzi, P.; Lenze, N.; Neumann, B.; Schoeller, W. W.; Stammler, H.-G. *Chem.—Eur. J.* **2006**, *12*, 5471–5480.

[11] (a) Park, J. W.; Seo, Y. S.; Cho, S. S.; Whang, D. M.; Kim, K. M.; Chang, T. Y. *J. Organomet. Chem.* **1995**, *489*, 23–25. (b) Zechel, D. L.; Foucher, D. A.; Pudelski, J. K.; Yap, G. P. A.; Rheingold, A. L.; Manners, I. *J. Chem. Soc., Dalton Trans.* **1995**, 1893–1899. (c) Ni, Y. Z.; Rulkens, R.; Pudelski, J. K.; Manners, I. *Macromol. Rapid Commun.* **1995**, *16*, 637–641. (d) Reddy, N. P.; Choi, N.; Shimada, S.; Tanaka, M. *Chem. Lett.* **1996**, 649–650. (e) MacLachlan, M. J.; Zheng, J.; Thieme, K.; Lough, A. J.; Manners, I.; Mordas, C.; LeSuer, R.; Geiger, W. E.; Liable-Sands, L. M.; Rheingold, A. L. *Polyhedron* **2000**, *19*, 275–289. (f) Calleja, G.; Carré, F.; Cerveau, G. *Organometallics* **2001**, *20*, 4211–4215. (g) Berenbaum, A.; Lough, A. J.; Manners, I. *Organometallics* **2002**, *21*, 4415–4424. (h) Bao, M.; Hatanaka, Y.; Shimada, S. *Chem. Lett.* **2004**, *33*, 520–521.

[12] Herberhold, M.; Bärtl, T. *Z. Naturforsch. B* **1995**, *50*, 1692–1698.

[13] (a) Seyferth, D.; Withers, H. P. *Organometallics* **1982**, *1*, 1275–1282. (b) Dong, T. Y.; Hwang, M. Y.; Wen, Y. S.; Hwang, W. S. *J. Organomet. Chem.* **1990**, *391*, 377–385. (c) Jäkle, F.; Rulkens, R.; Zech, G.; Foucher, D. A.; Lough, A. J.; Manners, I. *Chem.—Eur. J.* **1998**, *4*, 2117–2128. (d) Jäkle, F.; Rulkens, R.; Zech, G.; Massey, J.; Manners, I. *J. Am. Chem. Soc.* **2000**, *122*, 4231–4232. (e) Baumgartner, T.; Jäkle, F.; Rulkens, R.; Zech, G.; Lough, A. J.; Manners, I. *J. Am. Chem. Soc.* **2002**, *124*, 10062–10070.

[14] Utri, G.; Schwarzhans, K. E.; Allmaier, G. M. *Z. Naturforsch. B* **1990**, *45*, 755–762.

[15] (a) Brunner, H.; Klankermayer, J.; Zabel, M. *J. Organomet. Chem.* **2000**, *601*, 211–219. (b) Mizuta, T.; Onishi, M.; Miyoshi, K. *Organometallics* **2000**, *19*, 5005–5009. (c) Mizuta, T.; Imamura, Y.; Miyoshi, K. *Organometallics* **2005**, *24*, 990–996.

[16] Ieong, N. S.; Chan, W. Y.; Lough, A. J.; Haddow, M. R.; Manners, I. *Chem.—Eur. J.* **2008**, *14*, 1253–1263.

[17] Lund, C. L.; Schachner, J. A.; Quail, J. W.; Müller, J. *J. Am. Chem. Soc.* **2007**, *129*, 9313–9320.

[18] Robin, M. B.; Day, P. *Adv. Inorg. Chem. Radiochem.* **1967**, *10*, 247–422.

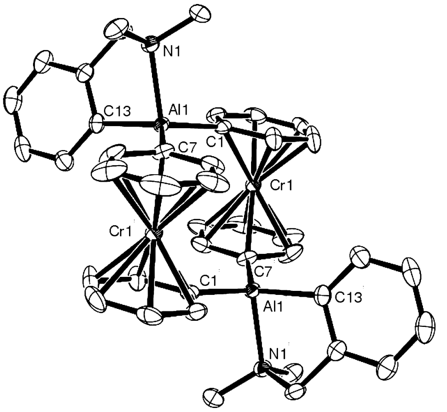

Figure 2. Molecular structure of **2a** with thermal ellipsoids at the 50% probability level. Hydrogen atoms are omitted for clarity. Selected atom−atom distances [angstroms] and bond angles [degrees]: Al1−N1 = 2.072(3), Al1−C1 = 1.972(4), Al1−C7 = 1.962(4), Al1−C13 = 1.978(4), Cr1−Cr1′ = 5.0866(10), C1−Al1−C7 = 121.22(16), N1−Al1−C13 = 85.78(14), C7−Al1−C13 = 120.44(16), C1−Al1−C13 = 113.65(16), C7−Al1−N1 = 103.15(14), C1−Al1−N1 = 101.95(14), α = 4.9(2).

is the first [1.1]chromarenophane known to date. **2a** crystallizes as an anti isomer with both NMe_2 donor groups in exo positions (Figure 1 and 2). Further structural details will be discussed below.

The poor solubility of **2a** made its separation from the simultaneously produced LiCl difficult, and, in addition, prevented investigations into metal−metal interactions in solution, hence, rendering electrochemical methods unsuitable. Therefore, we attempted to increase the solubility of the targeted [1.1]metallacyclophanes by using one-armed phenyl ligands Ar′ equipped with an additional alkyl group on the aromatic ring. From the ample possibilities, we picked an Ar′ derivative with one *t*Bu group para to the donor arm. Starting from commercially available p-(*tert*-butyl)benzylbromide (p-$tBuC_6H_4CH_2Br$) a known two-step synthesis yielded (p-*t*BuAr′)Li[19] [p-*t*BuAr′ = 5-*t*Bu-2-(Me_2NCH_2)C_6H_3] that was used to synthesize the new intramolecularly coordinated aluminum and gallium dichlorides **3a** and **3b**, respectively (eq 2). Expectedly, both species show ^{1}H and ^{13}C NMR spectra that can be interpreted as being caused by C_s symmetrical species. The ^{27}Al NMR shift of δ 131 for **3a** is very similar to δ 127 reported for the monomeric $Ar'AlCl_2$ (**1a**)[20] and shows that **3a** is a monomeric species with a 4-fold coordinated aluminum atom.

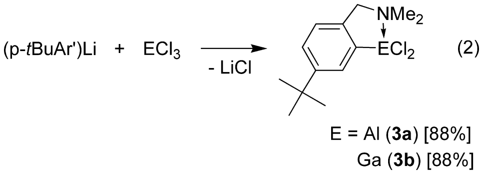

With the alane **3a** and the gallane **3b** in hand, novel [1.1]chromarenophanes and [1.1]molybdarenophanes with improved solubility were prepared through reactions with freshly dilithiated bis(benzene)chromium or -molybdenum (Scheme 1). The four [1.1]metallarenophanes **4a**,**b** and **5a**,**b** were isolated and purified by crystallizations from toluene solutions and crystals suitable for single crystal X-ray structural determination were obtained from benzene solutions (Figures 3 and 4, Table 1). According to ^{1}H NMR measurements of the reaction mixtures, the formation of the [1.1]metallacyclophanes proceeds relatively cleanly for this type of sensitive chemistry (estimated conversions of 80−90%). In all cases, we detected only small amounts of the parent bis(benzene)metal complex among the products. However, *N*,*N*,*N*′,*N*′-tetramethylethylenediamine (TMEDA), which is required for the dilithiation of the parent sandwich compounds, results in the formation of TMEDA·LiCl. It is the latter compound that is difficult to separate from the [1.1]metallacyclophanes, and, therefore, we isolated pure **4a**,**b** and **5a**,**b** in yields of only 20−30%.

Scheme 1

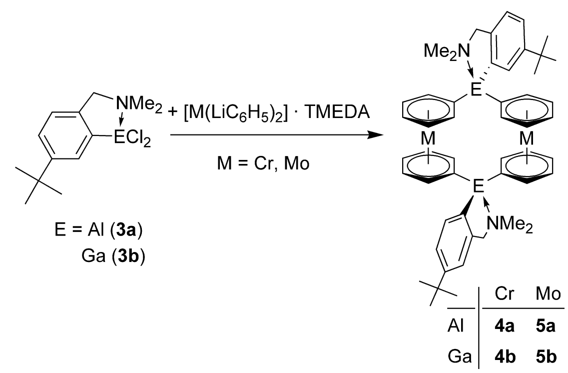

	Cr	Mo
Al	**4a**	**5a**
Ga	**4b**	**5b**

Solid-State Structures of 2a, 4a,b, and 5a,b. As in the case of the [1.1]ferrocenophanes investigated recently,[8,9] the new [1.1]chromarenophanes **2a** (Figure 2) and **4a,b** (Figure 3, Figure S1 in the Supporting Information) and the new [1.1]molybdarenophanes **5a**,**b** (Figure 4, Figure S2 in the Supporting Information) crystallize as anti isomers with the two NMe_2 donor groups in exo positions (Figure 1). All five species exhibit C_i point-group symmetries in the crystal lattice. The geometries around the bridging atoms can be best described as trigonal pyramids, with the three carbon atoms C1, C7, and C13 at the base and the nitrogen atom N1 at the tip of the pyramid. With respect to an ideal tetrahedron, these pyramids are flattened as it can be deduced from the sum over the three C−E−C angles (E = Al, Ga), which are 355.31 (**2a**), 354.14 (**4a**), 356.25 (**4b**), 354.12 (**5a**), and 355.79° (**5b**). Respective atom−atom distances in **2a**, **4a**,**b**, and **5a**,**b** are very similar; for example, the Cr−Cr distances are 5.9866(10), 5.9921(11), and 6.0251(6) Å for **2a**, **4a**, and **4b**, respectively, and the Mo−Mo distances are 5.9983(7) and 6.0277(6) Å for **5a** and **5b**, respectively. These metal−metal distances are larger for the gallium species as compared to the aluminum species, which is partly due to differences in E−C bond lengths: Ga1−C1 and Ga1−C7 bonds being slightly longer than respective Al−C bonds (Figures 3 and 4). Only the E−N donor bonds are very different for aluminum compared with gallium-bridged species, with Al−N donor bonds being shorter than Ga−N bonds (for **4a** and **4b**, the difference is 0.103(4) Å; for **5a** and **5b** it is 0.111(4) Å). Similar differences between E−N donor bond lengths were found for the [1.1]ferro-

---

(19) Cope, A. C.; Gourley, R. N. *J. Organomet. Chem.* **1967**, *8*, 527–533.
(20) Müller, J.; Englert, U. *Chem. Ber.* **1995**, *128*, 493–497.

Table 1. Crystal and Structural Refinement Data for **2a**, **4a**,**b**, and **5a**,**b**

	2a$\cdot$1/2C_6H_{12}	**4a**$\cdot$2C_6H_6	**4b**$\cdot$2C_6H_6	**5a**$\cdot$2C_6H_6[b]	**5b**$\cdot$2C_6H_6[b]
empirical formula	$C_{48}H_{56}Al_2Cr_2N_2$	$C_{62}H_{72}Al_2Cr_2N_2$	$C_{62}H_{72}Cr_2Ga_2N_2$	$C_{62}H_{72}$ $Al_2Mo_2N_2$	$C_{62}H_{72}Ga_2Mo_2N_2$
fw	818.91	1003.18	1088.66	1091.06	1176.54
cryst size, mm^3	0.20 × 0.20 × 0.12	0.12 × 0.10 × 0.10	0.20 × 0.18 × 0.15	0.13 × 0.13 × 0.10	0.08 × 0.08 × 0.050.71073
cryst. system, space group	monoclinic, $P2_1/c$	monoclinic, $P2_1/c$	monoclinic, $P2_1/c$	triclinic, $P\bar{1}$	triclinic, $P\bar{1}$
Z	2	2	2	1	1
a, Å	9.9117(9)	10.9626(9)	10.8428(2)	10.4377(4)	10.3451(5)
b, Å	19.9361(16)	19.3350(18)	19.4844(4)	11.6510(4)	11.6752(6)
c, Å	10.638(2)	12.4626(9)	12.4958(2)	11.6514(4)	11.6900(5)
α, deg	90	90	90	73.545(3)	73.917(3)
β, deg	112.322(5)	100.756(5)	100.6187	89.318(2)	89.550(3)
γ, deg	90	90	90	76.120(2)	76.774(2)
V, Å^3	1944.6(4)	2595.2(4)	2594.72(8)	1316.82(8)	1318.36(11)
ρ_{calcd}, mg/m^3	1.399	1.284	1.393	1.376	1.482
T, K	173(2)	173(2)	173(2)	173(2)	173(2)
μ_{calcd}, mm^{-1}	0.642	0.494	1.477	0.551	1.517
è range, deg	2.44 to 26.02	3.46 to 25.01	3.32 to 27.47	2.64 to 25.68	3.21 to 27.47
reflns collected/ unique	21561/3825	8155/4567	41481/5916	8528/4967	10303/6021
absorption correction	ψ-scan	none	ψ-scan	multiscan	multiscan
data/restraints/params	3825/96/273	4567/0/294	5916/0/313	4967/0/312	6021/0/312
GOF on F^2	1.052	1.032	1.072	1.069	1.059
final R indices [$I > 2\sigma(I)$][a]	0.0544	0.0653	0.0368	0.0453	0.0412
wR2 (all data)[a]	0.1387	0.1452	0.0848	0.1046	0.0941
largest diff. peak and hole, $\Delta\rho_{elect}$, Å^{-3}	0.975 and −0.761	0.278 and −0.304	0.326 and −0.376	0.462 and −0.660	0.690 and −0.801

[a] $R1 = [\Sigma||F_o| - |F_c||]/[\Sigma|F_o|]$ for $[F_o^2 > 2\sigma(F_o^2)]$, $wR2 = \{[\Sigma w(F_o^2 - F_c^2)^2]/[\Sigma w(F_o^2)^2]\}^{1/2}$ [all data]. [b] These compounds had been crystallized from C_6D_6 (Experimental Section). The deuterium atoms attached to the benzene solvent molecule were included as hydrogen atoms in the refinement. Chemical formula and derived quantities fw, ρ_{calcd}, μ_{calcd}, and $F(000)$ were not corrected.

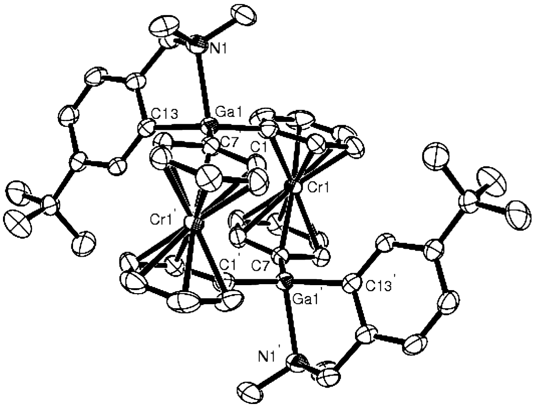

Figure 3. Molecular structure of **4b** with thermal ellipsoids at the 50% probability level. Hydrogen atoms are omitted for clarity. For an ORTEP plot of **4a**, see the Supporting Information. Selected atom−atom distances [angstroms] and bond angles [degrees] for **4a**: Al1−N1 = 2.089(4), Al1−C1 = 1.969(5), Al1−C7 = 1.978(5), Al1−C13 = 1.988(4), Cr1−Cr1′ = 5.9921(11), C1−Al1−C7 = 119.96(19), N1−Al1−C13 = 85.09(17), C7−Al1−C13 = 114.0(2), C1−Al1−C13 = 120.18(18), C7−Al1−N1 = 100.59(18), C1−Al1−N1 = 107.54(18), α = 3.21(14). Selected atom−atom distances [angstroms] and bond angles [degrees] for **4b**: Ga1−N1 = 2.192(2), Ga1−C1 = 1.980(2), Ga1−C7 = 1.979(2), Ga1−C13 = 1.984(2), Cr1−Cr1′ = 6.0251(6), C1−Ga1−C7 = 121.99(10), N1−Ga1−C13 = 83.41(9), C7−Ga1−C13 = 120.40(9), C1−Ga1−C13 = 113.86(10), C7−Ga1−N1 = 105.71(9), C1−Ga1−N1 = 99.04(9), α = 2.67(7).

cenophanes[8,9] mentioned before and are a testament of the higher Lewis acidity of aluminum compared with gallium for an amine donor.

For metallacyclophanes, a set of angles can be given to show the distortion with respect to the parent sandwich species.[21] The most illustrative angle is the tilt angle α which is the angle between the two intersecting planes defined by the carbon frameworks of the two coordinated π ligands. Aluminum- and gallium-bridged [1]metallacyclophanes exhibit α angles from 11.81(9)°[22] for an alumina[1]chromarenophane to 21.24(10)°[17] for an galla[1]molybdarenophane. [1.1]Metallacyclophanes are expected to be unstrained sandwich compounds, with tilt angles α close to 0°. For the new complexes **2a**, **4a**,**b** and **5a**,**b**, α angles of 4.9(2), 3.21(14), 2.67(7), 2.7(3), and 2.2(3)°, respectively, were determined. In all cases, the two planes intersect on the opposite side of the bridging atom, which could be indicated by adding a negative sign to all α angles.

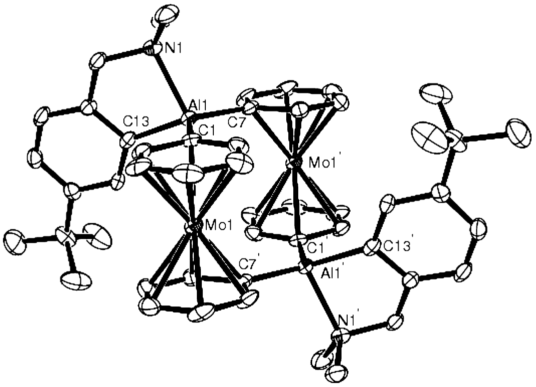

Figure 4. Molecular structure of **5a** with thermal ellipsoids at the 50% probability level. Hydrogen atoms are omitted for clarity. For an ORTEP plot of **5b**, see the Supporting Information. Selected atom−atom distances [angstroms] and bond angles [degrees] for **5a**: Al1−N1 = 2.096(3), Al1−C1 = 1.968(4), Al1−C7 = 1.968(4), Al1−C13 = 1.981(4), Mo1−Mo1′ = 5.9983(7), C1−Al1−C7 = 120.49(18), N1−Al1−C13 = 85.06(15), C7−Al1−C13 = 120.80(17), C1−Al1−C13 = 112.83(17), C7−Al1−N1 = 106.47(15), C1−Al1−N1 = 101.73(15), α = 2.7(3). Selected atom−atom distances [angstroms] and bond angles [degrees] for **5b**: Ga1−N1 = 2.207(3), Ga1−C1 = 1.978(3), Ga1−C7 = 1.967(3), Ga1−C13 = 1.983(3), Mo1−Mo1′ = 6.0277(6), C1−Ga1−C7 = 122.38(14), N1−Ga1−C13 = 83.08(13), C7−Ga1−C13 = 120.27(14), C1−Ga1−C13 = 113.14(14), C7−Ga1−N1 = 105.75(12), C1−Ga1−N1 = 100.32(12), α = 2.2(3).

NMR Spectroscopy of 2a, 4a,b, and 5a,b. ^1H and ^{13}C NMR spectra of **4a**,**b** and **5a**,**b** measured at ambient

---

(21) Herbert, D. E.; Mayer, U. F. J.; Manners, I. *Angew. Chem., Int. Ed.* **2007**, *46*, 5060–5081.

(22) Lund, C. L.; Schachner, J. A.; Quail, J. W.; Müller, J. *Organometallics* **2006**, *25*, 5817–5823.

temperatures, can be interpreted as being caused by time-averaged C_{2h} symmetrical species. For example, ^{1}H NMR spectra show one set of signals for the p-*t*BuAr′ ligands and five signals of equal intensities for the η^6-C_6H_5 moieties. In addition to the signal pattern, the ^{13}C NMR spectra show that the chemical shifts of the *ipso*-C atom of the η^6-C_6H_5 moieties at δ 76.0 (**4a**), 79.9 (**4b**), 76.6 (**5a**), and 79.8 (**5b**) are very similar to those of the parent compounds bis(benzene)chromium (δ 74.8)[23] and bis(benzene)molybdenum (δ 75.3).[24] The absence of an upfield shift clearly shows that the [1.1]metallacyclophanes are unstrained, corroborated by the molecular structures of the species in the solid state. As mentioned earlier, the aluminum-bridged [1.1]chromarenophane **2a** was not soluble in organic solvents anymore once it had crystallized; hence, we could not measure NMR spectra of the isolated product. However, a ^{1}H NMR spectrum was measured from the reaction mixture and showed a pattern comparable to those discussed for **4a**,**b** and **5a**,**b** (Experimental Section), but the low solubility of **2a** prevented the measurement of reliable ^{13}C NMR data.

Five-membered rings such as those present in the [1.1]metallarenophanes **2a**, **4a**,**b**, and **5a**,**b** show envelope conformations in the solid state. In solution, these rings would be expected to have conformational flexibility, and fast envelope inversions should result in five-membered rings which are C_s symmetrical on time average. Against this background, one expects that a C_i symmetrical [1.1]metallarenophane shows a C_{2h} symmetry in solution, meaning that our NMR results suggest that the molecular structures of **2a**, **4a**,**b**, and **5a**,**b** are similar in solution and in the crystal lattice.

As mentioned in the introduction, [1.1]ferrocenophanes had been coined “molecular acrobats”.[4] Consequently, we measured ^{1}H NMR spectra of **4a**,**b** and **5a**,**b** in $C_6D_5CD_3$ in the temperature range of −90 to 90 °C (500 MHz). Except for small shifts of signals, the high temperature spectra are very similar to those at ambient temperature. In the lower temperature range, a significant broadening of peaks between −70 and −90 °C occurred. However, even though some peaks are very broad at −90 °C, the signal pattern is still similar to that at ambient temperature. The low temperature spectra indicate that the molecular dynamics is slowed down with respect to the NMR time scale, but it is still fast enough at the lowest accessible temperature so that only one time-averaged C_{2h} symmetrical species is observed. One feasible dynamic process for [1.1]metallacyclophanes is a degenerate isomerization of one anti isomer to another anti isomer; a process comparable to a chair-to-chair isomerization of cyclohexane. If such a process would be occurring, with saturation transfer difference ^{1}H NMR experiments one should be able to see magnetization transfer from one ortho to the other ortho proton, similarly, from one meta to the other meta proton.[25] However, these experiments gave no indication that an anti-to-anti isomerization takes place even at temperatures of 80 °C (Experimental Section for details).

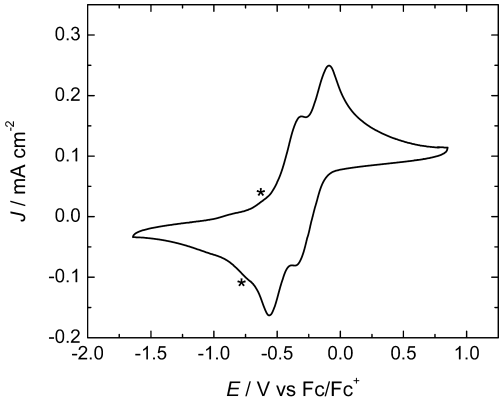

Figure 5. Cyclic voltammogram of **4b** in THF/0.1 M $[Bu_4N][PF_6]$ using a glassy carbon working electrode at a scan rate of 100 mV/s. The measured $E^{\circ\prime}$ for the two principal peaks are −0.440 and −0.225 V, respectively $[E^{\circ\prime} = 1/2(E_{pa} + E_{pc})]$.[26] The asterisk denotes a smaller set of voltammetric signals in the CV, which is due to small amounts of $[(C_6H_6)_2Cr]$.

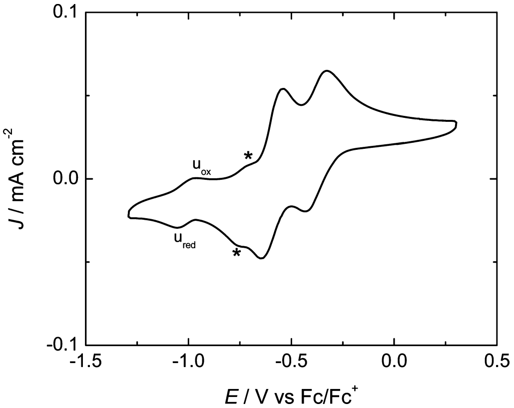

Figure 6. Cyclic voltammogram of **5b** in THF/0.1 M $[Bu_4N][PF_6]$ using a glassy carbon working electrode at a scan rate of 100 mV/s. The measured $E^{\circ\prime}$ for the two principal peaks is −0.600 and −0.380 V, respectively $[E^{\circ\prime} = 1/2(E_{pa} + E_{pc})]$.[26] The asterisk denotes a smaller set of voltammetric signals in the CV, which are due to small amounts of $[(C_6H_6)_2Mo]$. At very cathodic potentials (ca. −1.0 V), an additional redox process is observed (reversible couple denoted by u_{ox} and u_{red}).

Electrochemistry of 4a,b and 5a,b. Electrochemical measurements were undertaken for the four metallarenophanes to determine the extent of communication between the two transition-metal redox centers. In the first attempts, we used a small three-neck Schlenk flask with three electrodes inserted through septa (supporting information in ref 9). However, we did not obtain reproducible CVs; in particular, the two aluminum compounds showed only CVs of the parent bis(benzene) complexes, which suggested that moisture had degraded **4a** and **5a**, respectively. Consequently, all subsequent measurements were done inside a glovebox. Extra precautions were taken to dry the solvent THF and the electrolytes used (Experimental Section for details). With these efforts, we obtained reproducible data for the two gallium species **4b** and **5b** (Figures 5 and 6) but were unsuccessful in obtaining reproducible data for the respective aluminum compounds **4a** and **5a**. The measurements of the latter species indicated that significant amounts of the parent bis(benzene) complexes were always present in solution. Therefore, additional measurements of aluminum compounds

---

[23] Elschenbroich, C.; Koch, J. *J. Organomet. Chem.* **1982**, *229*, 139–158.

[24] Measured in C_6D_6 at 25 °C referenced to the signal at δ 128.00.

[25] Berger, S.; Braun, S. *200 and More NMR Experiments*, 3rd expanded ed.; Wiley-VCH: Weinheim, Germany, 2004; p 298.

4a and **5a** were performed using $[Bu_4N][BF_4]$ instead of $[Bu_4N][PF_6]$ as an electrolyte; however, their CVs varied significantly by this change. Furthermore, it seemed that the concentration of the parent sandwich compounds in a sample of **4a** or **5a** strongly influenced the position and intensities of the other oxidation and reduction waves and the obtained electrochemical data for **4a** and **5a** were inconclusive.

Figures 5 and 6 show the CVs of the gallium-bridged species **4b** and **5b**, respectively. **4b** shows two one-electron oxidation and two one-electron reduction waves. The shoulders at lower potential correspond to the redox couple of $[(C_6H_6)_2Cr]$ (asterisks in Figure 5). Similarly, species **5b** shows two redox couples which are due to one-electron events (Figure 6). As in the case of the chromium compound **4b**, the CV of the gallium-bridged molybdenum species **5b** reveals a pair of shoulders corresponding to the presence of $[(C_6H_6)_2Mo]$ (asterisks in Figure 6). In contrast to **4b**, however, an additional second reversible redox couple at high cathodic potentials was detected (u_{ox} and u_{red} in Figure 6), but we are unable to assign it to a compound. In summary, the two CVs can be interpreted consistently: both compounds, **4b** and **5b**, are oxidized at similar potentials compared to the respective parent sandwich compound $[(C_6H_6)_2M]$ (Supporting Information). According to the Robin−Day classification,[18] both species are class II compounds.

Conclusion

The first [1.1]metallarenophanes have been synthesized and fully characterized. The aluminum-bridged species (**2a**, **4a**, **5a**) and the gallium-bridged species (**4b**, **5b**) crystallize as anti isomers with the dimethylamino groups in exo positions (Figure 1). Structural parameters like atom−atom distances and bond angles are very similar in all five species. Expectedly, the E−N donor bonds are the only bonds that differ significantly: aluminum as the better Lewis acid for Me_2N donor groups possesses Al−N bonds that are shorter by 0.10 − 0.11 Å compared to the respective Ga−N bonds. ^1H and ^{13}C NMR spectra can be interpreted as being caused by C_{2h} symmetrical compounds. In contrast to their highly dynamic [1.1]metallocenophane cousins, these new [1.1]metallarenophanes do not show anti-to-anti isomerization in solution. [1.1]Metallacyclophanes can serve as model compounds to investigate metal−metal interactions; however, the extreme sensitivity of aluminum species **4a** and **5a** prevented us from obtaining reproducible electrochemical data. On the other hand, the gallium-bridged species **4b** and **5b** showed an expected class II behavior.

It is surprising that no other [1.1]metallarenophanes are known in the literature. The most common route for the synthesis of metallacyclophanes is the salt-metathesis between a dilithiated sandwich compound and an element dihalide.[21] In many cases, researchers used R_2SiCl_2; these compounds are commercially available and are very reactive toward nucleophilic substitutions. However, silicon in a bridging position of a [1.1]metallacyclophane would dictate approximately a tetrahedral angle for the $C_{ipso}-Si-C_{ipso}$ linkage. In [1.1]metallacyclophanes, there are two pairs of inner α protons, which are oriented toward each other (Figure 7). If all other structural parameters are kept constant, the distance between those α protons must be larger in [1.1]metallocenophanes, where two five-membered rings are linked, than in [1.1]metallarenophanes, where two six-membered rings are linked. It might be that, so far, steric repulsion between α protons prevented the formation of silicon-bridged [1.1]metallarenophanes. On the other hand, with aluminum- and gallium moieties in bridging positions the wider $C_{ipso}-E-C_{ipso}$ angles of around 120° reduce a possible repulsion between the α protons to allow the formation of [1.1]metallarenophanes [C1−E−C7 = 121.22(16) (**2a**), 119.96(19) (**4a**), 121.99(10) (**4b**), 120.49(18) (**5a**), 122.38(14) (**5b**); Figures 2, 3, and 4]. A second factor that might have contributed to the lack of reports about [1.1]metallarenophanes might be the low solubility of such compounds; **2a** showed unusual solubility properties in organic solvents. One can speculate that other [1.1]metallarenophanes might have been formed in salt-metathesis reactions but were not identified because of their insolubility.

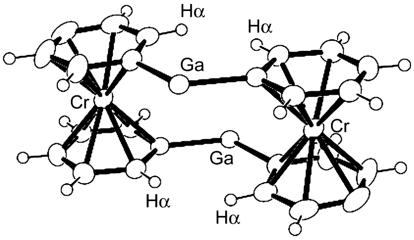

Figure 7. Illustration of two pairs of inner α protons pointing towards each other. Drawing is based on the experimentally determined molecular structure of compound **4b** (ligand p-*t*BuAr′ removed for clarity).

Experimental Section

Electrochemistry. A computer controlled system, consisting of a HEKA potentiostat PG590 (HEKA, Mahone Bay, NS, Canada) was used for the cyclic voltammetry experiments. Data was collected using a multifunction DAQ card (PCI 6251 M Series, National Instruments Austin, Texas) and in-house software written in the *LabVIEW* environment. Glassy carbon (BAS, 3 mm) was used as the working electrode. The quasi-reference electrode (QRE) was a silver wire ($E^{\circ\prime} = 0.645$ V vs Fc/Fc^+ with $E^{\circ\prime} = 1/2(E_{pa} + E_{pc})$; Supporting Information). All measurements were made against the QRE and subsequently rescaled to the ferrocene/ferrocenium formal potential[26] $E^{\circ\prime}$. A loop of gold wire was used as the auxiliary electrode. Before each measurement, 1 mM solutions of **4a**, **4b**, **5a**, and **5b** were freshly prepared in dry THF with 0.1 M $[Bu_4N][PF_6]$ as the supporting electrolyte. Extra efforts were undertaken to remove moisture and oxygen from the solvent. THF was first dried using a Braun Solvent Purification System and then filled into a 1L flask, which was part of a specialty Schlenk line, equipped with greaseless Young valves. To the so-predried THF, small amounts of 1,1-diphenylethylene and butyllithium were added, resulting in a red solution, which indicated the absence of moisture. By flask-to-flask condensation under reduced static pressure, a small amount of THF was condensed into a Schlenk tube from the THF reservoir flask. The inert gas (N_2 4.8) used for this Schlenk line was purified by conducting it through two columns before feeding it into the Schlenk line (one column equipped with a copper(I)

---

[26] Bard, A. J.; Faulkner, L. R. *Electrochemical Methods*, 2nd ed.; John Wiley & Sons, Inc.: New York, 2001, Chap. 6.

catalyst and one column equipped with 4 Å molecular sieves; both materials purchased from MBraun). A so-prepared Schlenk tube filled with freshly condensed THF was moved into the glovebox. The electrolytes were dried overnight under high vacuum ($[Bu_4N][PF_6]$ at 100 °C and $[Bu_4N][BF_4]$ at 70 °C). Unless otherwise specified, the scan rate for all of the CVs reported was 100 mV/s. All of the measurements were conducted inside a glovebox and taken at ambient temperature (24−25 °C).

Synthesis. All of the syntheses were carried out using standard Schlenk techniques. An MBraun glovebox ($O_2 < 1$ ppm, $H_2O < 1$ ppm) was used to manipulate the very sensitive bis(benzene) complexes including **2a**, **4a**,**b**, and **5a**,**b**. Solvents were dried using a MBraun solvent purification system and stored under nitrogen over 4 Å molecular sieves. All solvents for NMR spectroscopy were degassed prior to use and stored under nitrogen over 4 Å molecular sieves. $[Cr(C_6H_6)_2]$,[27] $[Mo(C_6H_6)_2]$,[17] $[Cr(LiC_6H_5)_2]\cdot$TMEDA,[28] $[Mo(LiC_6H_5)_2]\cdot$TMEDA,[29] [5-*t*Bu-2-(Me_2NCH_2)C_6H_3]Li,[19] and [2-(Me_2NCH_2)C_6H_4]$AlCl_2$ (**1a**)[20] were synthesized as described in the literature. ^1H, ^{13}C, and ^{27}Al NMR spectra were recorded on a Bruker 500 MHz Avance NMR spectrometer at 25 °C in C_6D_6, unless noted differently. ^1H chemical shifts were referenced to the residual protons of the deuterated solvent (δ 7.15 for C_6D_6); ^{13}C chemical shifts were referenced to the C_6D_6 signal at δ 128.00; ^{27}Al NMR spectra were referenced to $[Al(acac)_3]$ dissolved in C_6D_6 as an external standard. Mass spectra were measured on a VG 70SE ($m/z > 10\%$ are listed for signals of the most abundant ions). Elemental analyses were performed on a PerkinElmer 2400 CHN Elemental Analyzer using V_2O_5 to promote complete combustion.

For the saturation transfer difference experiments,[25] two spectra were measured, first a control spectrum and then one from a selective irradiation. Subtraction of the second from the first spectrum resulted in a difference spectrum displaying whether any protons exchange with the irradiated one. The pulse sequence used for the saturation transfer experiment was supplied by Bruker. **4b** (C_7D_8) was measured at 25 and 80 °C, and **5b** (C_6D_6) was measured at 25 °C without any detectable magnetization transfer. Selected parameters include presaturation time (d1 = 5.0 s), pulse power (pl14 = 95 dB), and number of data points (TD = 65536). T_1 times [s] for **5b** (C_6D_6): o-H = 0.6324; m-H = 1.315; p-H = 1.563; m-H = 1.490; o-H = 1.297.

Synthesis of [{2-(Me_2NCH_2)C_6H_4}Al(η^6-C_6H_5)$_2$Cr]$_2$ (2a). A slurry of $[Cr(LiC_6H_5)_2]\cdot$TMEDA (1.527 g, 4.541 mmol) in benzene (30 mL, 0 °C) was added to a solution of **1a** (1.016 g, 4.378 mmol) in benzene (10 mL, 0 °C). The cooling bath was removed, and the mixture was stirred for 30 min. LiCl was filtered off, and the filtrate containing the product was collected. The product was extracted with an additional (2 × 10 mL) of hot benzene from the LiCl filter cake, and the combined filtrates were reduced in volume to 10 mL, during which time a red precipitate formed that was separated by cannula transfer of the filtrate (0.201 g, 0.274 mmol). The mother liquor was stored at 6 °C to give additional red precipitate (0.138 g, 0.188 mmol). The total yield of **2a** was 0.339 g (21%). Single crystals for X-ray analysis were obtained from a highly diluted solution of **2a** in 1 mL of cyclohexane and 5 mL of THF at 25 °C. A ^1H NMR spectrum was obtained from the reaction mixture because dissolving the precipitate in common organic solvents was not successful. ^1H NMR: δ 1.71 (s, 12 H, NMe_2), 3.37 (s, 4H, CH_2), 4.26 (d, 4H, o-H), 4.29 (pst, 4H, m-H), 4.45 (pst, 4H, m-H), 4.62 (pst, 4H, p-H), 5.57 (d, 4H, o-H), 7.01 (d, 2H, 3-H), 7.37 (t, 2H, 4-H), 7.48 (t, 2H, 5-H), 8.47 (d, 2H, 6-H). MS (70 eV, EI +): *m/z* (%) 208 (21) $[Cr(C_6H_6)_2]^+$, 135 (27) $[C_9H_{13}N]^+$, 130 (24) $[C_6H_6Cr]^+$, 91 (15) $[C_7H_7]^+$, 78 (100) $[C_6H_6]^+$, 58 (33). Anal. Calcd for $C_{42}H_{44}Al_2Cr_2N_2$ (734.7674): C, 68.65; H, 6.04; N, 3.81. Found: C, 68.91; H, 6.12; N, 3.59.

Synthesis of [5-*t*Bu-2-(Me_2NCH_2)C_6H_3]$AlCl_2$ (3a). A solution of $AlCl_3$ (2.477 g, 18.58 mmol) in Et_2O (30 mL, −80 °C) was added to a solution of [5-*t*Bu-2-(Me_2NCH_2)C_6H_3]Li (3.670 g, 18.60 mmol) in Et_2O (20 mL, −80 °C) followed by stirring at room temperature for 6 h. The suspension was filtered to remove LiCl, the filtrate was collected, and the remaining product was extracted with an additional 30 mL of Et_2O from the LiCl filter cake. All volatiles were removed from the combined filtrates, and subsequent sublimation of the resulting solid under high vacuum (110 °C) gave **3a** as a white crystalline solid (4.692 g, 88%). ^1H NMR: δ 1.19 (s, 9H, *t*Bu), 1.87 (s, 18 H, 2 $SiMe_3$), 3.05 (s, 6H, NMe_2), 6.73 (d, 1H, 3-H), 7.32 (d, 1H, 4-H), 7.86 (s, 1H, 6-H). ^{13}C NMR: δ 31.5 (*t*Bu), 45.3 (NMe_2), 65.3 (CH_2), 124.4 (3-C), 126.7 (4-C), 133.6 (6-C), 139.9 (2-C, *ipso*-C), 150.5 (5-C, *ipso*-C). ^{27}Al NMR: δ 131 ($w_{1/2}$ = 2500 Hz). MS (70 eV, EI +): *m/z* (%): 287 (26) $[M]^+$, 272 (100) $[M - CH_3]^+$, 191 (45) $[MH - AlCl_2]^+$, 147 (30) $[MH - NMe_2 - AlCl_2]^+$, 140 (34), 131 (50) $[M - NMe_2 - AlCl_2 - CH_3]^+$, 117 (12) $[M - CH_2 - NMe_2 - AlCl_2 - CH_3]^+$, 91 (19) $[C_7H_7]^+$, 58 (52) $[C_4H_{10}]^+$. Anal. Calcd for $C_{13}H_{20}AlCl_2N$ (288.1921): C, 54.18; H, 6.99; N, 4.86. Found: C, 54.11; H, 6.80; N, 5.03.

Synthesis of [5-*t*Bu-2-(Me_2NCH_2)C_6H_3]$GaCl_2$ (3b). A solution of $GaCl_3$ (3.2315 g, 18.352 mmol) in Et_2O (40 mL, −80 °C) was added to a solution of [5-*t*Bu-2-(Me_2NCH_2)C_6H_3]Li (3.6133 g, 18.319 mmol) in toluene (40 mL, −80 °C) followed by stirring at room temperature for 16 h. LiCl was filtered off, the filtrate collected, and remaining product was extracted with CH_2Cl_2 (2 × 20 mL) from LiCl filter cake. The combined filtrates were reduced to dryness under vacuum to give a white solid. Subsequent sublimation under high vacuum (120 °C) gave **3b** as a white crystalline solid (5.331 g, 88%). ^1H NMR: δ 1.14 (s, 9H, *t*Bu), 1.88 (s, 18 H, 2 $SiMe_3$), 2.95 (s, 6H, NMe_2), 6.69 (d, 1H, 3-H), 7.26 (d, 1H, 4-H), 7.73 (s, 1H, 6-H). ^{13}C NMR: δ 31.4 (*t*Bu), 45.3 (NMe_2), 64.5 (CH_2), 125.2 (3-C), 126.9 (4-C), 132.5 (6-C), 138.0 (2-C, *ipso*-C), 151.6 (5-C, *ipso*-C). MS (70 eV, EI +): *m/z* (%): 314 (10) $[M - CH_3]^+$, 191 (81) $[MH - GaCl_2]^+$, 175 (10) $[MH - CH_3 - GaCl_2]^+$, 147 (57) $[MH - NMe_2 - GaCl_2]^+$, 132 (20) $[M - CH_2 - NMe_2 - GaCl_2]^+$, 117 (19) $[M - CH_2 - NMe_2 - GaCl_2 - CH_3]^+$, 105 (11) $[C_8H_9]^+$, 92 (19) $[C_7H_8]^+$, 58 (100) $[C_4H_{10}]^+$. Anal. Calcd for $C_{13}H_{20}AlCl_2N$ (330.9336): C, 47.18; H, 6.09; N, 4.23. Found: C, 46.86; H, 6.19; N, 4.19.

Synthesis of [{5-*t*Bu-2-(Me_2NCH_2)C_6H_3}Al(η^6-C_6H_5)$_2$Cr]$_2$ (4a). A slurry of $[Cr(LiC_6H_5)_2]\cdot$ TMEDA (1.142 g, 3.396 mmol) in benzene (30 mL, 0 °C) was added to a solution of **3a** (0.976, 3.39 mmol) in benzene (10 mL, 0 °C). The cooling bath was removed, and the mixture was stirred for 1 h. All volatiles were removed in vacuum. The product was extracted with toluene (2 × 10 mL), filtered to remove LiCl, and storage of the filtrate at −25 °C led to the formation of dark-red crystals of **4a** (0.425 g, 30%). Single crystals for X-ray analysis were obtained from benzene at 6 °C. ^1H NMR: δ 1.58 (s, 18H, *t*Bu), 1.75 (s, 12 H, NMe_2), 3.42 (s, 4H, CH_2), 4.30 (br. s, 8H, o-H, m-H), 4.48 (pst, 4H, p-H), 4.73 (pst, 4H, m-H), 5.77 (d, 4H, *o*-H), 7.05 (d, 2H, 3-H), 7.50 (d, 2H, 4-H), 8.69 (s, 2H, 6-H). ^{13}C NMR: δ 32.1 (*t*Bu), 46.8 (NMe_2), 67.1 (CH_2), 75.0 (*p*-C), 75.6 (*m*-C or *o*-C), 76.0 (*ipso*-C), 76.5 (*m*-C), 80.6 (*o*-C), 81.9 (*o*-C or *m*-C), 123.9 (3-C), 124.7 (4-C), 135.0 (6-C), 142.8 (2-C, *ipso*-C), 149.2 (5-C, *ipso*-C). MS (70 eV, EI +):

---

[27] *Synthetic Methods of Organometallic and Inorganic Chemistry*; Herrmann, W. A., Ed.; Georg Thieme Verlag Stuttgart: New York, 1997; Vol. 8.

[28] Elschenbroich, C.; Hurley, J.; Metz, B.; Massa, W.; Baum, G. *Organometallics* **1990**, *9*, 889–897.

[29] Green, M. L. H.; Treurnicht, I.; Bandy, J. A.; Gourdon, A.; Prout, K. *J. Organomet. Chem.* **1986**, *306*, 145–165.

m/z (%) 208 (43) $[Cr(C_6H_6)_2]^+$, 191 (100) $[C_{13}H_{21}N]^+$, 175 (10) $[C_{12}H_{17}N]^+$, 154 (12), 147 (71) $[C_{11}H_{15}]^+$, 134 (14) $[C_9H_{12}N]^+$, 132 (25) $[C_{10}H_{12}]^+$, 130 (49) $[C_6H_6Cr]^+$, 119 (11), 117 (27) $[C_9H_9]^+$, 105 (11). Anal. Calcd for $C_{50}H_{60}Al_2Cr_2N_2$ (846.9801): C, 70.90; H, 7.14; N, 3.31. Found: C, 70.70; H, 6.98; N, 3.12.

Synthesis of $[\{5\text{-}t\text{Bu-2-}(Me_2NCH_2)C_6H_3\}Ga(\eta^6\text{-}C_6H_5)_2Cr]_2$ (4b). A slurry of $[Cr(LiC_6H_5)_2]$ · TMEDA (1.072 g, 3.188) in benzene (30 mL) was added to a solution of **3b** (1.073 g, 3.242 mmol) in benzene (10 mL, 0 °C). The cooling bath was removed, and the mixture was immediately warmed to ambient temperature and stirred for 1 h. All volatiles were removed in vacuum. The dark-red product was extracted with toluene (2 × 10 mL) and filtered to remove LiCl. The filtrate was concentrated to 10 mL and kept at −25 °C to yield dark-red crystals of **4b** (0.410 g, 28%). Single crystals suitable for X-ray analysis were obtained from benzene at 6 °C. ^{1}H NMR: δ 1.57 (s, 18H, 2 *t*Bu), 1.72 (s, 12H, 2 NMe_2), 3.35 (s, 4H, 2 CH_2), 4.28 (pst, 4H, *m*-H), 4.31 (d, 4H, *o*-H), 4.44 (pst, 4H, *p*-H), 4.73 (pst, 4H, *m*-H), 5.73 (d, 4H, o-H), 7.08 (d, 2H, 3-H), 7.46 (d, 2H, 4-H), 8.58 (s, 2H, 6-H). ^{13}C NMR: δ 32.1 (*t*Bu), 46.6 (NMe_2), 66.7 (CH_2), 75.0 (*p*-C), 75.8 (*m*-C), 76.6 (*m*-C), 79.9 (*ipso*-C), 80.7 (*o*-C), 81.6 (*o*-C), 124.2 (3-C), 124.4 (4-C), 134.1 (6-C), 142.2 (2-C, *ipso*-C), 149.5 (5-C, *ipso*-C). MS (70 eV, EI +): *m/z* (%): 208 (19) $[Cr(C_6H_6)_2]^+$, 191 (100) $[C_{13}H_{21}N]^+$, 175 (10) $[C_{12}H_{17}N]^+$, 147 (71) $[C_{11}H_{15}]^+$, 134 (13) $[C_9H_{12}N]^+$, 132 (25) $[C_{10}H_{12}]^+$, 130 (22) $[C_6H_6Cr]^+$, 119 (13), 117 (32) $[C_9H_9]^+$, 115 (13), 105 (13). Anal. Calcd for $C_{50}H_{60}Cr_2Ga_2N_2$ (932.463): C, 64.40; H, 6.49; N, 3.00. Found: C, 64.42; H, 5.89; N, 3.02.

Synthesis of $[\{5\text{-}t\text{Bu-2-}(Me_2NCH_2)C_6H_3\}Al(\eta^6\text{-}C_6H_5)_2Mo]_2$ (5a). A slurry of $[Mo(LiC_6H_5)_2]$ · TMEDA (1.192 g, 3.135 mmol) in benzene (30 mL) was added to a solution of **3a** (0.914 g, 3.17 mmol) in benzene (10 mL, 0 °C). The cooling bath was removed, and the mixture was stirred for 1 h resulting in a red-brown solution. All volatiles were removed in vacuum. The product was extracted with toluene (4 × 5 mL), and the solution was filtered to remove LiCl. The filtrate was concentrated to 10 mL and kept at −25 °C to yield green crystals, which were washed with benzene (2 × 3 mL) and dried on high vacuum to give **5a** (0.428 g, 29%). Single crystals for X-ray analysis were obtained from C_6D_6 at 25 °C from an NMR tube. ^{1}H NMR: δ 1.51 (s, 18H, 2 *t*Bu), 2.01 (s, 9H, 2 NMe_2), 3.45 (s, 4H, 2 CH_2), 4.38 (d, 4H, *o*-H), 4.46 (pst, 4H, *m*-H), 4.86 (pst, 4H, *p*-H), 4.96 (pst, 4H, *m*-H), 5.82 (d, 4H, *o*-H), 6.99 (d, 2H, 3-H), 7.43 (d, 2H, 4-H), 8.24 (s, 2H, 6-H). ^{13}C NMR: δ 32.0 (*t*Bu), 47.1 (NMe_2), 67.3 (CH_2), 74.1 (*p*-C), 76.3 (*m*-C), 76.6 (*ipso*-C), 77.4 (*m*-C), 81.8 (*o*-C), 81.9 (*o*-C), 123.8 (3-C), 124.6 (4-C), 134.7 (6-C), 142.6 (2-C, *ipso*-C), 148.9 (5-C, *ipso*-C). MS (70 eV, EI +): *m/z* (%): 191 (100) $[C_{13}H_{21}N]^+$, 190 (88) $[C_{13}H_{20}N]^+$, 175 (10) $[C_{12}H_{17}N]^+$, 154 (16), 147 (73) $[C_{11}H_{15}]^+$, 134 (11) $[C_9H_{12}N]^+$, 132 (25) $[C_{10}H_{12}]^+$, 119 (10), 117 (24) $[C_9H_9]^+$, 105 (12). Anal. Calcd for $C_{50}H_{60}Al_2Mo_2N_2$ (934.8679): C, 64.24; H, 6.47; N, 3.00. Found: C, 64.03; H, 6.33; N, 3.32.

Synthesis of $[\{5\text{-}t\text{Bu-2-}(Me_2NCH_2)C_6H_3\}Ga(\eta^6\text{-}C_6H_5)_2Mo]_2$ (5b). A slurry of $[Mo(LiC_6H_5)_2]$ · TMEDA (1.071 g, 2.817) in benzene (30 mL) was added to a solution of **3b** (0.917 g, 2.77 mmol) in benzene (10 mL, 0 °C). The cooling bath was removed, and the mixture was stirred for 1 h, resulting in a red-brown solution. All volatiles were removed in vacuum. The product was extracted with toluene (4 × 5 mL) and filtered to remove LiCl. The filtrate was concentrated to 10 mL and kept at −25 °C to yield green crystals, which were washed with benzene (2 × 3 mL) and dried to give **5b** (0.283 g, 20%). Single crystals for X-ray analysis were obtained from C_6D_6 at 25 °C from an NMR tube. ^{1}H NMR: δ 1.23 (s, 18 H, 2 *t*Bu), 1.97 (s, 12 H, 2 NMe_2), 3.38 (s, 4H, 2 CH_2), 4.40 (d, 4H, o-H), 4.47 (t, 4H, m-H), 4.82 (t, 4H, p-H), 4.98 (t, 4H, m-H), 5.83 (d, 4H, o-H), 7.02 (d, 2H, 3-H), 7.39 (d, 2H, 4-H), 8.13 (s, 2H, 6-H). ^{13}C NMR: δ 32.0 (*t*Bu), 46.9 (NMe_2), 66.8 (CH_2), 74.5 (*p*-C), 76.5 (*m*-C), 77.5 (*m*-C), 79.8 (*ipso*-C), 81.5 (*o*-C), 81.7 (*o*-C), 124.1 (4-C), 124.2 (3-C), 133.8 (6-C), 142.0 (2-C, *ipso*-C), 149.2 (5-C, *ipso*-C). MS (70 eV, EI +) *m/z* (%): 414 (10) $[C_{25}H_{30}GaN]^+$, 338 (100), 337 (51) $[C_{19}H_{26}GaN]^+$, 336 (93) $[C_{19}H_{25}GaN]^+$, 296 (21), 294 (21), 293 (18) $[C_{17}H_{20}Ga]^+$, 191 (23) $[C_{13}H_{21}N]^+$, 190 (19) $[C_{13}H_{20}N]^+$, 147 (16) $[C_{11}H_{15}]^+$. Anal. Calcd for $C_{50}H_{60}Ga_2Mo_2N_2$ (1020.3508): C, 58.86; H, 5.93; N, 2.75. Found: C, 58.65; H, 5.43; N, 2.49.

Crystal Structure Determination. Crystal data of **2a**, **4a**,**b**, and **5a**,**b** were collected at −100 °C on a Nonius Kappa CCD diffractometer, using monochromated Mo Kα radiation (λ = 0.71073 Å) at −100 °C. An initial orientation matrix and cell was determined by φ scans, and the X-ray data were measured using φ and ω scans.[30] Data reduction was performed with *HKL DENZO* and *SCALEPACK* software.[31] Structures were solved by direct methods (*SIR-97*)[32] and refined by full-matrix least-squares methods on F^2 with *SHELX-97*.[33] Unless otherwise stated, the non-hydrogen atoms were refined anisotropically; hydrogen atoms were included at geometrically idealized positions but not refined. The isotropic thermal parameters of the hydrogen atoms were fixed at 1.2 times that of the preceding carbon atom. Neutral atom scattering factors for non-hydrogen atoms and anomalous dispersion coefficients are contained in the *SHELXTL-NT 6.14* program library.[34] Crystallographic data are summarized in Table 1. *ORTEP-3 for Windows*[35] was used for molecular graphics and *PLATON*[36] was used to prepare material for publication.

For **2a**, a disordered cyclohexane molecule in the lattice was modeled with restraints to hold its geometry. The cyclohexane molecule is lying on a symmetry center in the lattice, which generates the superimposed mirror image of the cyclohexane molecule and results in some very short H···H distances (as short as 1.84 Å) to hydrogen atoms in the **2a** molecule. For **4b**, the disordered benzene molecule in the structure was modeled as a rigid molecule with anisotropic displacement parameters.

5a,**b** were crystallized from C_6D_6, which was incorporated into their lattices. The deuterium atoms attached to the benzene solvent molecule were included as hydrogen atoms at geometrically idealized positions and were not refined. The chemical formula and the derived quantities fw, ρ_{calcd}, μ_{calcd}, and $F(000)$ were not corrected, to account for the presence of these deuterium atoms.

Acknowledgment. We thank G. A. Orlowski (University of Guelph) and H.-B. Kraatz (University of Western Ontario) for their help with electrochemical measurements in the initial stage of the project. We thank K. Brown (University of Saskatchewan) for NMR measurements. We thank the Natural Sciences and Engineering Research Council of Canada (NSERC Discovery Grant, J.M.), the Department of

---

(30) Nonius, B. V. *Nonius Collect*; *Delft, The Netherlands*, 1998.

(31) Otwinowski, Z.; Minor, W. In *Macromolecular Crystallography*; Part A; Carter, C. W., Sweet, R. M., Eds.; Academic Press: London, 1997; Vol. *276*, pp 307−326..

(32) Altomare, A.; Burla, M. C.; Camalli, M.; Cascarano, G.; Giacovazzo, C.; Guagliardi, A.; Moliterni, A. G. G.; Polidori, G.; Spagna, R. *J. Appl. Crystallogr.* **1999**, *32*, 115–119.

(33) Sheldrick, G. M. *SHELXL97−2: Program for the Solution of Crystal Structures; University of Göttingen: Göttingen, Germany*, 1997.

(34) *SHELXTL-NT 6.14: Program Library for Structure Solution and Molecular Graphics*; 2000.

(35) Farrugia, L. J. *J. Appl. Crystallogr.* **1997**, *30*, 565.

(36) Spek, A. L. *PLATON, A Multipurpose Crystallographic Tool; University of Utrecht: The Netherlands*, 2001.

Chemistry, the Saskatchewan Structural Sciences Centre, and the University of Saskatchewan for their generous support. We thank the Canada Foundation for Innovation (CFI) and the government of Saskatchewan for funding of the X-ray and NMR facilities in the Saskatchewan Structural Sciences Centre (SSSC).

Supporting Information Available: ORTEP plots for compounds **4a** and **5b**; X-ray crystallographic data for **2a**, **4a**,**b**, and **5a**,**b** in CIF format; CVs of [$(C_5H_5)_2Fe$], [$(C_6H_6)_2Cr$], and [$(C_6H_6)_2Mo$] with respect to the silver quasi-reference electrode. This material is available free of charge via the Internet at http://pubs.acs.org. Crystallographic data for all of the structures in this article have been deposited with the Cambridge Crystallographic Data Centre, under CCDC 675591 (**2a**), CCDC 675592 (**4a**), CCDC 675593 (**4b**), and CCDC 675594 (**5a**), and CCDC 675595 (**5b**). These data can be obtained free of charge from The Cambridge Crystallographic Data Centre via www.ccdc.cam.ac.uk/data_request/cif.

IC800336F